A Simple Partitioning Model for Reversibly Cross-Linked Polymers and Application to the Poly(vinyl alcohol)/Borate System ("Slime")

Elizabeth T. Wise and Stephen G. Weber*

Department of Chemistry and Materials Research Center, University of Pittsburgh, Pittsburgh, Pennsylvania 15260

Received January 17, 1995; Revised Manuscript Received August 25, 1995®

ABSTRACT: Gels of some polymeric polyols cross-linked by borate can be liquefied by certain low molecular weight polyols. As the gels respond with some molecular selectivity, we view them as model smart materials. In an effort to gain a quantitative understanding of such chemically responsive polymer systems, we have studied the gelation of atactic poly(vinyl alcohol) (PVA) by borate and have at the same time determined the equilibrium concentration of borate in free solution in the presence of various concentrations of polymer. The standard approach to the determination of the distribution of borate among its various forms—free borate, free boric acid, borate bound to a diol (monodiol), and borate bound to a pair of diols (didiol)—is to use the relevant chemical equilibria and the diol concentration dependence of the borate distribution. This is not appropriate for polymer systems. We have developed a model that uses simple geometrical arguments to define the volume fraction of a polymer solution in which two chains are close enough to be cross-linked. This volume is used with the borate chemical equilibria to define how many borate cross-links there are. From this model, which is generally applicable to chemically reversible gels, experimentally observed gel points and equilibrium concentrations of free borate are predicted when using reasonable input parameters. Furthermore, the model also predicts the mean chain length between cross-links.

Introduction

Smart materials respond to their physical or chemical environment.[1–16] In the presence of a stimulus, they recognize, discriminate, and react to produce some useful effect. This ability of inanimate matter to both *sense* and *actuate* is a characteristic of living systems and it allows for high performance with low energy requirements. Chemically sensitive smart materials are far less studied than physically sensitive smart materials.

Chemically sensitive, reversible gel-forming polymer systems will form the basis of soft, lifelike smart materials. In this kind of system, the chemical sensitivity arises from the presence of reversible chemical cross-links. These reversible gels can be formed and destroyed because a change in conditions (temperature, pH, solvent, ionic strength, concentration of cross-linker) can alter the extent of cross-linking. The most interesting and useful systems are those in which the cross-link-forming reaction shows some chemical selectivity based on molecular recognition, such as a lectin-containing polymer that responds to saccharides,[17] an acrylate that responds to Cu(II),[18] and polyol-containing polymers that response to borate.[19–35] We are particularly interested in the latter systems as they show primitive smart material behavior.[36] The chemistry relevant to the polyol–borate systems is shown in Scheme 1. In reaction 1 borate reacts with a diol unit on a polymer to form a monodiol. In reaction 2, the monodiol reacts with a second diol unit to form a didiol. If both diol units are on the same chain, the didiol is an intramolecular cross-link, while if the diol units are on different chains, the cross-link is intermolecular.

Among the types of phase transitions that polyol–borate systems undergo are bulk phase separation into a concentrated polymer gel and a dilute polymer solution and a transition from homogeneous solution to homogeneous gel. The former has been investigated.[20,36–38] In particular, Pezron *et al.*[37,39] have used a Flory model[40] that takes into account both charge repulsion and formation of intrachain cross-links to predict and explain quantitatively phase separation. Of equal interest is the quantitative explanation of behavior near the gelation threshold. Pezron *et al.*[22,23] have demonstrated recently that behavior in polymeric diol–borate systems is different from the small-molecule case for polymer concentrations below C^*.[20–23,36,37,41–43] In this case, the concentration of didiols (intramolecular cross-links) is linearly related to the polymer concentration, whereas in the analogous reaction of a small diol, the concentration of didiols depends quadratically on the small-molecule concentration. The difference arises because the diol concentration in the vicinity of a polymeric diol chain is not dependent on the bulk polymer concentration. The formation of cross-links is not dependent upon the *global* ligand concentration, but rather the *local* concentration of ligands around an already formed 1:1 complex.

Scheme 1

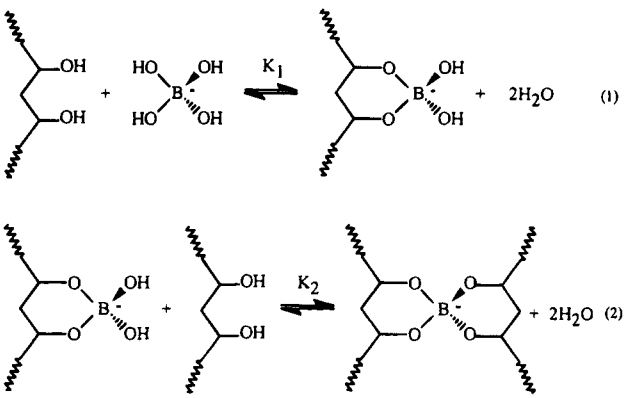

* Author to whom correspondence should be addressed.

® Abstract published in *Advance ACS Abstracts,* November 1, 1995.

0024-9297/95/2228-8321$09.00/0

In order to treat the PVA–borate–sugar system[19,36,38,44,45] as a primitive smart material, we must have a quantitative understanding of the relationship between borate ion concentration and material properties, particularly near the gel point. While there has been some work on an analogous system, in which metal ions cross-link polymers,[41] there is not a good model for the prediction of material properties from the concentrations of the polymer and cross-linker for any reversible gel. Existing models[20,39,42,46,47] are based on the simple equilibrium expressions for analogous small molecules.[48–50] It is our goal to comprehend how component concentrations affect network structure and, thereby, govern the physical properties. We have developed a quantitative model that describes the gelation behavior of the PVA–borate system as a first step toward this aim.

Experimental Section

Materials. Poly(vinyl alcohol) (99% mol hydrolyzed, number-average molecular weight (M_n), 54 000) was obtained from Polysciences, Inc. (Warrington, PA) and used as received; the supplier reported the polydispersity of the polymer to be very close to 2. We measured it and found it to be 1.81. The following chemicals were purchased from standard sources and used without further purification: sodium tetraborate decahydrate (borax), D-mannitol, sodium azide, sucrose, glycerol, potassium bromide, sodium bicarbonate, sodium hydroxide, sodium acetate, monobasic potassium phosphate, 2-butanol, 1- and 2-propanol, ethanol, and 4,5-dihydroxy-2,7-naphthalenedisulfonic acid. Doubly deionized water (Millipore Milli-Q Type I Reagent Grade water system) was used in all solutions.

Sample Preparation. PVA was added slowly to bicarbonate buffer (pH 10.0, 1.50 mM azide, ionic strength = 60.0 mM) with stirring. Subsequent slow heating to 86 °C aided dissolution. The mixture was allowed to stir for 4 h. PVA solutions were then gravity filtered. To determine the actual polymer concentration, a small amount of two PVA/water solutions were allowed to dry, and the remaining solid polymer was weighed. The dissolution technique resulted in a concentration that was 5.5% lower than that calculated based on the total weight of polymer taken. All polymer concentrations reported here are the weighed quantity × 0.945/volume of solvent.

Samples for the viscosity measurements were produced by mixing appropriate volumes of PVA and borax. Gelation occurred within an average of 20 s. Samples were stored immediately in amber bottles and tested approximately 2 weeks later.

Samples for boron determinations were dialyzed for 1 week at 30.0 °C. Spectra/Por 1 dialysis bags (MW cutoff 6000–8000) containing 20 mL aliquots of PVA solution (0.0482–0.244 M in diol) were immersed in stoppered Erlenmeyer flasks filled with 100 mL of borax solution (0.200–2.50 mM). Control runs employed dialysis bags containing buffer only.

Infrared Spectroscopy. A few PVA grains were mixed with 0.080 g of dried potassium bromide; the mixture was pressed to yield a transparent disk. An IBM IR/32 spectrometer scanned the sample 32 times in the 400–4000 cm^{-1} range. The stereochemistry of the hydroxyl groups was determined according to the equation of Fujii.[51]

Viscometry. The low-viscosity polymer solutions used to determine intrinsic viscosity were tested in a Cannon–Fenske calibrated viscometer tube (Fisher Scientific, size 100) immersed in a 30 °C water bath. 1-Butanol was used to calibrate the instrument. The measured kinematic viscosity was multiplied by density to give absolute viscosity.

Viscosities of the PVA–borate systems were measured by a Physica viscometer using a concentric-cylinder geometry (Viscolab FP10) connected to a Haake temperature bath set at 30.0 °C. For low-viscosity samples, a cylinder was calibrated with 1-butanol, 1- or 2-propanol, and ethanol. For high-viscosity samples, a cylinder was calibrated with glycerol. The responses of the solutions were generally linear (i.e., shear stress varied linearly with shear rate), while those of the gels were noisy and irreproducible.

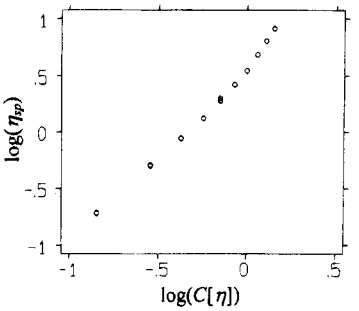

Figure 1. Log of specific viscosityt, η_{sp}, as a function of the log of the reduced concentration, $C[\eta]$. $C^* = 1.29$ g/dL is the concentration at which a transition occurs due to polymer–polymer entanglements.

Table 1. Viscosity, η (cP)

[boron] (mM)	[diol] (M) 0.122	0.146	0.170	0.19	0.219	0.244
0.840	2.42	3.21	4.15	5.90	6.61	10.4
0.952	2.42	3.36	4.47	6.38	7.35	11.0
1.43	2.66	3.75	5.47	10.3	29.2	37.7
1.70	2.71				662	
1.91	PS[a]	4.81	9.46	27.5	922	2.63×10^3
2.10				136		
2.38	PS	PS	PS	1.13×10^3	1.21×10^3	3.14×10^3
2.80					4.77×10^3	
3.20					5.46×10^3	
3.30						1.18×10^4

[a] Phase separation.

Boron Determination. A flow injection analysis (FIA) system using UV–visible detection[52] was constructed to determine free boron concentration in the dialyzed samples. The reagent, chromotropic acid (4,5-dihydroxy-2,7-naphthalenedisulfonic acid in pH 7.5 0.5 M sodium acetate), demonstrated a UV spectral change in the presence of borate. The decreased absorbance of CTA upon complexation with borate was detected by a Gilson UV–visible spectrophotometer set at 361 nm. The reagent is light-sensitive and was protected by covering the reservoir with aluminum foil. Triplicate injections were performed at each concentration level; the response was linear over the concentration range of 0–6000 μg/L total boron.

Results

PVA was characterized by infrared spectroscopy, which indicated that 46.0% of the diol groups are in the isotactic configuration. Therefore, as expected for an atactic polymer, approximately half of the coordinating sites are available for complexation.

C^*, the overlap concentration, may be determined experimentally by plotting the log of the specific viscosity against the log of the reduced concentration $C[\eta]$,[53] where $[\eta] = 0.650$ dL/g is the intrinsic viscosity (see Figure 1). C^* was determined by the intersection of the tangents to the two linear regions in Figure 1 and found to be 1.29 g/dL or 0.146 M diol.

A total of 91 PVA–borate samples were prepared for either viscosity measurements or boron determination. Of these 91, 12 were gels, 40 were two-phase systems, and 39 were liquids. The viscosities of the liquids and gels are listed in Table 1. If there is a coexistence region between gel and liquid, it is small. Figure 2 shows the state of the resulting system as a function of boron concentration and diol concentration at 30 °C. Polymer concentration is given in units of diol concentration

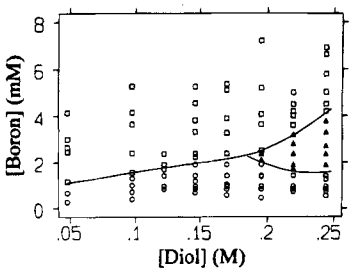

Figure 2. Phase diagram of the PVA–borate system at 30 °C: (□) two phase; (○) liquid; (▲) gel.

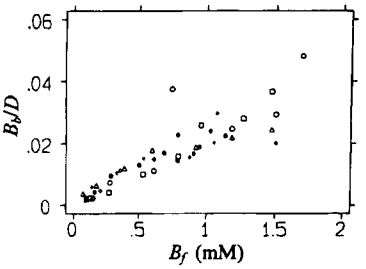

Figure 3. Fraction of borate complexed with diol plotted against equilibrium concentrations of free boron for six diol concentrations (○) 0.0482, (□) 0.0973, (△) 0.146, (◇) 0.170, (+) 0.195, and (○) 0.244 M). Control of the free boron concentration allows for manipulation of the physical properties.

because it is the diol that coordinates with borate. At low concentrations of each component, the solution is viscous. Gel formation is observed when a certain diol concentration is reached. At relatively high concentrations of boron, two phases are formed; an elastic material separates from a relatively inviscid liquid. These materials will be studied in the future.

Free boron concentration was determined by flow injection analysis of solutions in equilibrium with PVA inside dialysis tubing. The equilibrium concentrations of free boron are shown in Figure 3. The fraction of borate that is coordinated with diol is plotted against free boron concentration for six polymer concentrations.

Discussion

Model. Recently, Pezron *et al.*[22] have shown that the formation of *intra*molecular cross-links in a system similar to the one studied here is not well described by equilibrium expressions developed for small molecules. Their observation on borate/poly(glyceryl methacrylate) is that the formation of didiols in the same polymer chain is independent of polymer concentration. They argued convincingly that the relevant determinant of the probability of the formation of a didiol is not the concentration of polymer as it is visualized in the laboratory, but rather the local concentration of diols around an already formed monodiol complex. This is influenced by chain stiffness and other polymer attributes, but not the bulk polymer concentration. Their analysis was restricted to concentrations below C^*.

We have developed a simple model for the prediction of chemical and physical properties of smart materials that starts with the well-understood small-molecule formalism but applies it to the polymer case in a way that is physically reasonable but distinct from the small-molecule case. In the polymer case, there are *competing* equilibria that pull on the monodiol: *intra*molecular formation of didiol and *inter*molecular formation of didiol. In the small-molecule case, the former is generally precluded. In the polymer case, the two equilibria compete on an entropy basis, and the intramolecular didiol is more likely unless two polymer molecules are already enmeshed.

The model that we develop here bears a resemblance to micelle partitioning.[54] Individual polymer chains exist in a spherical solvent volume. The borate is viewed as partitioning among three volumes of solvent: polymer-free solvent, solvent associated with single polymer chains, and solvent associated with regions in which the spheres of two polymer chains overlap. The distribution of unbound borate depends only on the volumes of the three regions. Once the borate ion is in either of the regions containing a polymer chain, it can bind as a monodiol, as an *intra*molecular didiol, or as an *inter*molecular didiol. The binding depends on the polymer concentration in each region, but this is not related to the mass per volume concentration of the polymer solution as a whole; rather it is related to the solvent-swollen molar volume of the polymer.

In order to predict the distribution of borate, it is necessary to determine several volumes into which the borate partitions. There is polymer-free solvent, solvent in the spherical domain of a polymer chain, and solvent in domains where two spheres overlap. In determining how much of the volume contains two polymer chains (those domains where two spheres overlap), it is necessary to know the distance between the spheres and the radius of each sphere.

The distance between the spheres is governed by the concentration of the polymer. The separation distance depends upon the geometrical disposition of the polymer chains. Because of the simplicity and convenience of the cubic and body-centered geometry, we have chosen these arrangements to describe our polymer system. These descriptions are not realistic views because a polymer system is random, but the arrangements are simple systems with reasonable coordination numbers and easily obtainable volumes. If they are arranged in a cubic lattice, then the separation distance, d, is just

$$d = (n_p)^{-1/3} \tag{3}$$

where n_p is the polymer number density. If the geometry is body-centered cubic (bcc), then the separation distance is

$$d = \frac{3^{1/2}}{2}\left(\frac{2}{n_p}\right)^{1/3} \tag{4}$$

As a factor $3^{1/2}2^{-2/3}$ is 1.091, this aspect is not a critical part of the problem. A more important distinction is the coordination number. In the cubic array, each polymer chain has six nearest neighbors. In the bcc, each chain has eight nearest neighbors. In practice, we have found that the results of the computation are not strongly dependent on subtle differences between the geometry of the spatial arrangement of the polymer-containing units. Thus, except for a brief mention below, we will ignore this factor.

The radius of each sphere encompassing a polymer chain can be estimated using the random walk of a freely rotating chain have a fixed valence angle of 109.5°.[40] At this angle, the root-mean-square of the radius of gyration is a simple function of the number, m, and length, l, of valence bonds:[40]

$$R_{g,rms} = m^{1/2}l/3^{1/2} \tag{5}$$

If we take R_g to be 3 times $R_{g,rms}$, a value of 13.9 nm is obtained.

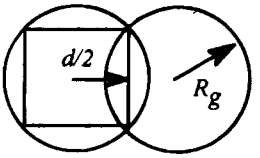

Figure 4. Overlapping polymer/solvent spheres showing the separation distance, d, and the radius of gyration, R_g.

A more reliable value of R_g can be found through an experimentally derived relationship with C^*:[55]

$$R_g = \left(\frac{M_w}{(4/3)\pi C^* N_{Av}}\right)^{1/3} \quad (6)$$

where $M_w = 1.8M_n$ is the weight-average molecular weight and N_{Av} is Avogadro's number. When C^* is 1.29 g/dL and M_w is 108 000, R_g is 14.4 nm.

Our model is based on particle *counting* and, thus, is dependent upon the number-average molecular weight. The model assumes a monodisperse polymer. In order for the model to be internally consistent, R_g must be determined from eq 6 using the number-average molecular weight. When C^* is 1.29 g/dL and $M_w = M_n$ is 59 800, R_g is 12.3 nm.

The overlap volume between two spheres may be estimated. This volume is pictured in Figure 4. We now define a dimensionless distance, z, which is proportional to d, $z = d/(2R_g)$. When z is greater than one, there is no overlap.

The following calculations are based on the bcc geometry. The unit cell contains two polymer chains, one central chain with 1/8 of each of its 8 nearest neighbors. When the spheres of volume $V_s = (4/3)\pi R_g^3$ (in cm^3) begin to overlap because the polymer concentration is increasing, they form the discus-shaped overlapping region pictured in Figure 4. In one unit cell, there are 8 of these volumes. Each discus-shaped region has a volume

$$V_{discus} = V_s\left(\frac{z^3}{2} - \frac{3z}{2} + 1\right) \quad (z \le 1) \quad (7)$$

$$f_{o2} = 8\frac{V_{discus}}{V_s} \quad (8)$$

The fraction f_{o2} is that fraction of a single sphere volume that is the eight overlapping regions from the nearest neighbors. In the bcc, there are 6 next nearest neighbors. The next nearest neighbors are the central spheres in adjacent unit cells. They are centered at a distance that is $2/\sqrt{3}$ times the center-to-center distance of the nearest neighbors. If we define the variable z_{nn}, which is $(2/\sqrt{3})z$, then the volume of the discus-shaped entities formed from the overlap of next nearest neighbors is

$$V_{discus,nn} = V_s\left(\frac{z_{nn}^3}{2} - \frac{3z_{nn}}{2} + 1\right) \quad (z_{nn} \le 1) \quad (9)$$

$$f_{o2nn} = 6\frac{V_{discus,nn}}{V_s} \quad (10)$$

The fraction f_{o2nn} is that fraction of a sphere volume that is the six overlapping regions from the next nearest neighbors. Let us now calculate three volumes in the polymer solution: V_0 is the volume of solution containing no polymer (region 0), V_1 is the volume containing a single polymer chain (region 1), and V_2 is the volume containing two polymer chains (region 2, the discus-shaped regions).

To calculate V_0, we need to determine how much of the unit cell volume is taken up by the spheres of polymer/solvent, and the remainder is free solvent. The unit cell volume V_{uc} is

$$V_{uc} = 2/n_p \quad (11)$$

The number of unit cells is just $V_t n_p/2$, where V_t is the total experimental volume. Each unit cell has two spheres, so these volumes must be subtracted from the total. When the spheres overlap, subtraction of the total volume of the two spheres counts the overlap twice; thus we cound one sphere's total volume, and one sphere decremented by the volumes of the discus-like pieces that correspond to overlap.

$$V_0 = \frac{V_t n_p}{2}\left(\frac{2}{n_p} - V_s\left(2 - f_{o2} - \frac{f_{o2nn}}{2}\right)\right) = V_t\left(1 - n_p V_s\left(1 - \frac{f_{o2}}{2} - \frac{f_{o2nn}}{4}\right)\right) \quad (12)$$

V_1 is calculated similarly,

$$V_1 = n_p V_s V_t\left(1 - f_{o2} - \frac{f_{o2nn}}{2}\right) \quad (13)$$

as is V_2

$$V_2 = n_p V_s V_t\left(\frac{f_{o2}}{2} + \frac{f_{o2nn}}{4}\right) \quad (14)$$

We now have quantitative definitions for the three volumes, V_0, V_1, and V_2. To obtain the solvent volume therein, we must correct for the volume of the polymer chain itself. When spheres do not overlap, the fraction of a sphere containing a single chain that is polymer is

$$f_p = \bar{V}_p/\bar{V}_s \quad (15)$$

where $\bar{V}_p$ is the molar volume of unsolvated polymer and $\bar{V}_s$ is the molar volume of the sphere (i.e., $N_{Av}V_s$). Then, the corrected volumes are

$$V_1 = n_p V_s V_t\left(1 - f_{o2} - \frac{f_{o2nn}}{2}\right)(1 - f_p) \quad (16)$$

$$V_2 = n_p V_s V_t\left(\frac{f_{o2}}{2} + \frac{f_{o2nn}}{4}\right)(1 - 2f_p) \quad (17)$$

The factor of 2 arises in the latter expression as the fraction of space occupied by polymer in an overlap region must be $2f_p$.

We now have divided the polymer solution into volumes into which borate can partition. Once borate is in a volume, it can bind to polymer. The binding is governed by equilibria such as eqs 18–20.

$$B^- + D \rightleftharpoons BD^- \qquad K_1 = [BD^-]/([B^-][D]) \quad (18)$$

$$BD^- + D \rightleftharpoons BD_2^- \qquad K_2 = [BD_2^-]/([BD^-][D]) \quad (19)$$

$$B^- + 2D \rightleftharpoons BD_2^- \qquad K_{12} = [BD_2^-]/([B^-][D]^2) \quad (20)$$

There is an important consequence of the model that we have developed that concerns the diol concentration.

In region 1, the molar diol concentration is just the number of moles of diol equivalents divided by the sphere volume.

$$D_s = \frac{1000M_n}{V_s N_{Av} M_d} \tag{21}$$

where M_d is the equivalent diol formula weight (88). In region 2, the diol concentration is just $2D_s$. Note that we have not made any correction for the percent *cis*-diols in the atactic polymer.

The borate is then distributed among the various regions. We account for all the borate through mass balance. The total borate quantity (moles) is given as

$$B_t = \{(V_0 + V_1 + V_2)f_{H^+} + V_1(D_s K_1 + D_s{}^2 K_1 K_2) + V_2(2D_s K_1 + 4D_s{}^2 K_1 K_2)\}[B^-] \tag{22}$$

where $f_{H^+} = 1 + [H^+]/K_a$ accounts for the boron in the form of boric acid. In practice, we compute $[B^-]$, the concentration of borate in region 0 as $B_t/\{...\}$; where $\{...\}$ is the quantity in braces in eq 22. As parameters, we use K_1, K_2, and R_g. From $[B^-]$, the number of cross-links per polymer chain, X, can be determined as the number of didiols in region 2 normalized to the number of polymer chains.

$$X = \frac{V_2(4D_s{}^2 K_1 K_2)[B^-]}{n_p V_t N_{Av}{}^{-1}} \tag{23}$$

When $X \geq 1$, according to the Flory–Stockmayer criterion, the solution gels.

Before applying the model, it is worthwhile to consider a couple of points. The major point is that the polymer concentration relevant to formation of monodiols and didiols is the *local* concentration within regions 1 and 2. The D_s and $D_s{}^2$ terms in eq 22 are constants for a particular solvent/polymer combination. They do not refer to the diol concentration in the solution as a whole. The polymer concentration dependence of the cross-link density depends on the polymer number density, n_p, through its influence on the polymer–polymer spacing an the volume of the overlap region. Therefore, the macroscopically observed dependence of the amount of borate bound to polymer on the polymer concentration results from the influence of n_p and f_{o2} on V_0, V_1, and V_2.

The second point is the importance of the dimensionless quantity $n_p V_s$. Imagine the total solvent volume being divided into spheres of volume V_s. When $n_p V_s$ is unity, the mean occupancy of a sphere by a polymer chain is unity. This concentration corresponds to C^*.[47] Clearly, for $n_p V_s > 1$ overlap of polymer chains is significant, while for $n_p V_s \ll 1$ it is not. When $n_p V_s$ is equal to the void fraction corresponding to a packed bed of spheres in the geometry of the system, then the spheres, and by implication the polymer chains in the spheres, just are touching.

A final point concerns $n_p V_s \geq 2$. Under these conditions, the overlapping volumes begin to overlap each other. Such multiple overlapping regions are hard to describe with certainty. The geometrical problem is complicated and dependent on the spatial arrangement of the spheres. Furthermore, it is not at all obvious that if s hypothetical spheres overlap, it means that s real polymer chains come together to create a region in which the local concentration of polymer is s times the local concentration of polymer in an isolated sphere. Thus, the model as it now stands probably loses accuracy for $n_p V_s \geq 2$.

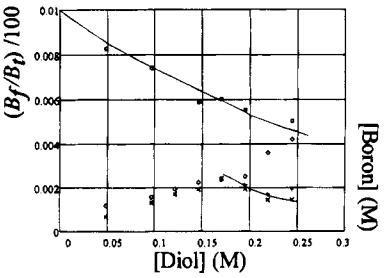

Figure 5. Fit of model to gelation (lower portion) and borate distribution (upper portion). In the lower portion, the symbols represent the following experimental observations: (×) edge of the liquid region; (+) lower edge of the gel region; (◇) lower edge of the two-phase region; the solid line represents the predicted gel point, i.e., when $X = 1$, for the, bcc-sphere geometry (M_n = 59 800, $K_1 = 2.4$, $K_2 = 4.7$, $R_g = 12.3$ nm, $c_n = 8$, $c_{nn} = 6$). In the upper portion, □ shows the measured free fraction of borate (ordinate × 100 = free fraction of borate), and the solid line illustrates the prediction for the bcc sphere.

Application to PVA/Borate Gelation. We will apply the foregoing model in two cases. It will be used to understand the liquid–gel transition quantitatively. It will then be used qualitatively in a discussion of the data of Pezron *et al.*[22] from their study of the similar borate/poly(glyceryl methacrylate) system.

In order to apply the model, we determine concentrations of borate and polymer at which $X = 1$. There are two parameters that we alter: K_1 and K_2. As the liquid–gel transition is only suggested by the data, it is hard to do a statistically rigorous fit to the data. As a consequence, we have chosen to obtain qualitatively reasonable predictions of the liquid–gel transition and simultaneously of the free concentration of borate, which was determined experimentally. An example is shown in Figure 5. Two plots are superimposed in this figure. In the lower portion, the experimentally determined liquid and gel regions are delineated by the symbols, and the theoretical line is seen to fall between the regions. The theoretical line for the gel point only applies to the boundary between a homogeneous gel and a viscous solution; thus it is restricted to the range where the experimental results show this behavior. In the upper portion, the measured concentration of free borate is shown, as is the prediction. The data are adequately represented by the model. The parameters determined by the model depend upon the exact model used, but as stated above, the geometry dependence is slight. For four different geometries, we obtain (mean ± 95% confidence interval) $K_1 = 2.8 \pm 0.3$ and $K_2 = 3.2 \pm 1.1$ (M_n = 59 800 and R_g = 12.3 nm).

Literature values of K_1 are on the same order of magnitude as our results, but data across the literature were obtained under variations in polymer tacticity and lack of control of the pH (which controls how much of the boron exists as the active species: borate). Furthermore, K_2 has not been measured accurately because bulk concentration of polymer was used in eqs 18–20.

It is instructive to view the distribution of volumes graphically (see Figure 6). As polymer concentration increases, separation distance decreases. At the point where the region 0 and region 1 curves cross, the average occupancy of a sphere, if the total volume of solution were divided into volumes V_s, is 0.5; that is, $n_p V_s = 0.5$. At a somewhat higher concentration, $n_p V_s$ becomes equal to the void fraction; depending on

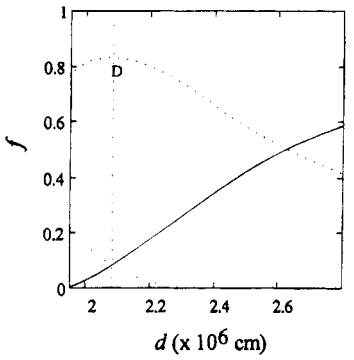

Figure 6. f is the fraction of volume corresponding to each region (unitless), d is the polymer–polymer separation distance (in units of 10^6 cm) ((—) region 0; (···) region 1; (- - -) region 2), and D is the separation distance at C^*. Parameters as in Figure 5.

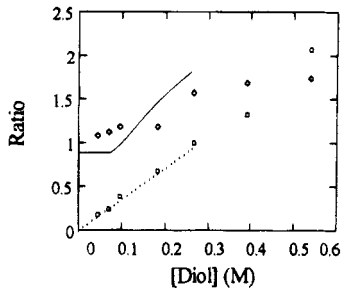

Figure 7. Ratio of [didiol]/[monodiol] and [monodiol]/[free] predicted by the model ((■) and (- - -)) and experimentally by Pezron *et al.* ((◇) and (□), respectively). Model parameters: $M_d = 160$, $M_p = 90\,000$, $K_1 = 3.6$, $K_2 = 7$, $R_g = 12.1$ nm, $c_n = 6$.

geometry, this will be in the range 0.6–0.7. At this point, overlap begins, and region 2 becomes nonzero. At the point where the region 2 and region 0 curves cross, n_pV_s is unity.

Application to Poly(glyceryl methacrylate). Let us now turn to the application of the model to the data of Pezron *et al.*[22] for the similar system borate poly(glyceryl methacrylate). The nice aspect of this system is that didiol and monodiol complexes are distinguishable by ^{11}B NMR. These authors observed that, for $C < C^*$, the ratio of [didiol]/[monodiol] vs [diol] is roughly constant. The small-molecule equilibria predict a straight line through 0,0. Our model prediction is shown in Figure 7. It is qualitatively in complete agreement with the data of Pezron *et al.*

The fit of the monodiol-to-free borate ratio is very good and the predicted didiol-to-monodiol ratio shows the same trend as the experimental data. The discrepancy in the latter fit may be due to polydispersity. A distribution in molecular weight will result in a gradual overlapping of polymer/solvent volume elements as polymer concentration increases. The model, which is monodisperse, shows a sharp transition in the didiol-to-monodiol ratio where the volume elements begin to overlap. Furthermore, polydispersity should cause a shift in the onset of gelation to higher diol concentrations. Larger spheres that overlap will give a larger overlap volume and, thus, lead to a higher probability of interchain cross-link formation, while smaller spheres may not overlap at all. The intermolecular cross-links will be "localized" or concentrated in areas of high overlap volume. Thus, the average number of cross-links per polymer chain (X) may still be one (theoretical gel point), but the network would no longer be continuous. The monodisperse model defines gelation when $X = 1$. In a polydisperse system, gelation will occur for $X > 1$.

Conclusion

In macromolecular, polydentate ligands, intramolecular cross-linking is much more likely than intermolecular cross-linking in dilute solutions. At concentrations approaching and beyond C^*, intermolecular cross-links compete effectively, and gelation can result. Of interest in the development of smart materials are three-component systems in which a low molecular weight ligand competes with polymer for cross-linker. It is essential for quantitative evaluation of such systems to be able to describe the chemical equilibria in such a way that the macromolecular nature of the polymeric ligand is correctly included. This has been done in the current treatment by allowing the cross-linking agent to partition among various volumes, the magnitudes of which are defined by polymer properties and concentration, and then react within each volume with the available diols at their local concentration.

Acknowledgment. Financial support of this work by the Army Research Office, the Materials Research Center at the University of Pittsburgh, and EBI Sensors, Inc., are gratefully appreciated. We thank Felicia Tang for the molecular weight determination.

References and Notes

(1) Amato, I. *Science* **1992**, *255*, 284.
(2) Filisko, F. E. *Chem. Ind.* **1992**, *10*, 370.
(3) Newnham, R. E. *MRS Bull.* **1993**, *18* (4), 24.
(4) Osada, Y.; Ross-Murphy, S. B. *Sci. Am.* May 1993, 82.
(5) Studt, T. *R&D Mag.* April 1992, 55.
(6) Tanaka, T. *Sci. Am.* **1981**, *244* (1), 124.
(7) Uchino, K. *MRS Bull.* **1993**, *18* (4), 42.
(8) Hathaway, K. B.; Clark, A. E. *MRS Bull.* **1993**, *18* (4), 34.
(9) Osada, Y.; Gong, J. P.; Ohnishi, S.; Sawahata, K.; Hori, H. *J. Macromol. Sci., Chem.* **1991**, *A28* (11–12), 1189.
(10) Wayman, C. M. *MRS Bull.* **1993**, *18* (4), 49.
(11) Filisko, F. E.; Armstrong, W. F. Eur. Pat. Applo. EP 265,-252, 1988.
(12) DeRossi, Danilo, Ed. *Polymer Gels: Fundamentals and Biomedical Applications.* Plenum Press: New York, 1991; pp 147–157.
(13) Okahata, Y.; Noguchi, H.; Seki, T. *Macromolecules* **1987**, *20*, 15.
(14) Barbucci, R.; Casolaro, M.; Magnani, A. *J. Controlled Release* **1991**, *17*, 79.
(15) Weber, A. Sensor for Determining the Concentration of a Biochemical Species. International Patent Application No. PCT/DK86/00126, Nov 17, 1986.
(16) Cussler, E. L.; Stokar, M. R.; Vaarberg, J. E. *AIChE J.* **1983**, *30*, 578.
(17) Kokufata, E.; Zhang, Y.; Tanaka, T. *Nature* **1991**, *351*, 302.
(18) Ricka, J.; Tanaka, T. *Macromolecules* **1985**, *18*, 83.
(19) Deuel, H.; Neukom, H.; Weber, F. *Nature* **1948**, *161*, 96.
(20) Kurokawa, H.; Shibayama, M.; Ishimaru, T.; Nomura, S.; Wu, W.-l. *Polymer* **1992**, *33* (10), 2182.
(21) Shibayama, M.; Yoshizawa, H.; Kurokawa, H.; Fujiwara, H.; Nomura, S. *Polymer* **1988**, *29*, 2066.
(22) Pezron, E.; Leibler, L.; Ricard, A.; Lafuma, F.; Audebert, R. *Macromolecules* **1989**, *22*, 1169.
(23) Pezron, E.; Leibler, L.; Lafuma, F. *Macromolecules* **1989**, *22*, 2656.
(24) Pezron, E.; Ricard, A.; Lafuma, F.; Audebert, R. *Macromolecules* **1988**, *21*, 1121.
(25) Ochiai, H.; Fujino, Y.; Tadokor, Y.; Murakami, I. *Polymer* **1980**, *21*, 485.
(26) Ochiai, H.; Kurita, Y.; Murakami, I. *Makromol. Chem.* **1984**, *185*, 167.
(27) Ochiai, H.; Shimizu, S.; Tadokoro, Y.; Murakami, I. *Polym.* **1981**, *22*, 1456.
(28) Matsuzawa, S.; Yamaura, K.; Tanigami, T.; Somura, T.; Nakata, M. *Polym. Commun.* **1987**, *28*, 105.
(29) Shibayama, M.; Sato, M.; Kimura, Y.; Fujiwara, H.; Nomura, S. *Polymer* **1988**, *29*, 336.

(30) Sinton, S. W. *Macromolecules* **1987**, *20*, 2430.
(31) Sato, T.; Tsujii, Y.; Fukuda, T.; Miyamoto, T. *Macromolecules* **1992**, *25*, 3890.
(32) Righetti, P. G.; Snyder, R. S. *Appl. Theor. Electrophor.* **1988**, *1*, 53.
(33) Maerker, J. M.; Sinton, S. W. *J. Rheol.* **1986**, *30*, 77.
(34) Savins, J. G. *Rheol. Acta* **1968**, *7*, 87.
(35) Cheng, A. T. Y.; Rodriguez, F. *J. Appl. Polym. Sci.* **1981**, *26*, 3895.
(36) Wise, E. T.; Weber, S. G. *Polym. Prepr. (Am. Chem. Soc., Div. Polym. Chem.)* **1993**, *34*, 215.
(37) Pezron, E.; Leibler, L.; Ricard, A.; Audebert, R. *Macromolecules* **1988**, *21*, 1126.
(38) Nickerson, R. F. *J. Appl. Polym. Sci.* **1971**, *15*, 111.
(39) Leibler, L.; Pezron, E.; Pincus, P. A. *Polymer* **1988**, *29*, 1105.
(40) Flory, Paul J. *Principles of Polymer Chemistry*; Cornell University Press: Ithaca, NY, 1953.
(41) Menjivar, J. A. *Polym. Mater. Sci. Eng.* **1984**, *51*, 88.
(42) Allain, C.; Salomé, L. *Macromolecules* **1990**, *23*, 981.
(43) Pezron, E.; Ricard, A.; Leibler, L. *J. Polym. Sci., B: Polym. Phys.* **1990**, *28*, 2445.
(44) Casassa, E. Z.; Sarquis, A. M.; Van Dyke, C. H. *J. Chem. Educ.* **1986**, *63*, 57.
(45) Deuel, H.; Neukom, H. *Makromol. Chem.* **1949**, *3*, 13.
(46) Kesavan, S.; Prud'homme, R. K. *Macromolecules* **1992**, *25*, 2026.
(47) de Gennes, P.-G. *Scaling Concepts in Polymer Physics*; Cornell University Press: Ithaca, NY, 1979.
(48) Hoffstetter-Kuhn, S.; Paulus, A.; Gassmann, E.; Widmer, H. M. *Anal. Chem.* **1991**, *63*, 1541.
(49) Kankare, J. J. *Anal. Chem.* **1973**, *45*, 2050.
(50) Knoeck, J.; Taylor, J. K. *Anal. Chem.* **1969**, *41*, 1730.
(51) Fujii, K.; Mochizuki, T.; Imoto, S.; Ukida, J.; Matsumoto, M. *J. Polym. Sci.* **1964**, *2*, 2327.
(52) Lussier, T.; Gilbert, R.; Hubert, J. *Anal. Chem.* **1992**, *64*, 2201.
(53) Graessley, W. *Adv. Polym. Sci.* **1974**, *16*, 1.
(54) Nowick, J. S.; Chen, J. S.; Noronha, G. *J. Am. Chem. Soc.* **1993**, *115*, 7636.
(55) Oberthür, R. C. *Makromol. Chem.* **1978**, *179*, 2693.

MA950043D